



ELSEVIER

Available online at [www.sciencedirect.com](http://www.sciencedirect.com)

SCIENCE @ DIRECT®

Journal of volcanology  
and geothermal research

Journal of Volcanology and Geothermal Research 132 (2004) 241–251

[www.elsevier.com/locate/jvolgeores](http://www.elsevier.com/locate/jvolgeores)

# Modeling of the steady-state temperature field in lava flow levées

Francesca Quarenì<sup>a,\*</sup>, Andrea Tallarico<sup>b</sup>, Michele Dragoni<sup>c</sup>

<sup>a</sup> INGV-OV, via D. Creti 12, 40128 Bologna, Italy

<sup>b</sup> Dipartimento di Geologia e Geofisica, Università di Bari, Bari, Italy

<sup>c</sup> Dipartimento di Fisica, Università di Bologna, viale Berti Pichat 8, 40127 Bologna, Italy

Received 20 February 2002; received in revised form 24 February 2002; accepted 15 July 2003

## Abstract

The rationale of lava flow deviation is to prevent major damage, and, among the possible techniques, the opening of the flow levées has often been demonstrated to be suitable and reliable. The best way to open the levées in the right point, in order to obtain the required effect, is to produce an explosion in situ, and it is then necessary to map with the highest precision the temperature field inside the levées, in order to design a safe and successful intervention. The levées are formed by lava flows due to their non-Newtonian rheology, where the shear stress is lower than the yield stress. The levées then cool and solidify due to heat loss into the atmosphere. In this work we present analytical solutions of the steady-state heat conduction problem in a levée using the method of conformal mapping for simple geometrical shapes of the levee cross-section (triangular or square). Numerical solutions are obtained with a finite-element code for more complex, realistic geometries.

© 2003 Elsevier B.V. All rights reserved.

## 1. Introduction

Lava flows are erupted at the Earth's surface during effusive volcanic activity, and their morphology and dynamics are mainly ruled by the typically non-Newtonian rheological behavior of lava. Field measurements of physical properties of lavas (e.g. Shaw et al., 1968; Pinkerton and Sparks, 1978) show their pseudo-plastic behavior, due to a partial crystallization in the magmatic suspension, determining a finite yield strength, which must be exceeded in order to flow, and

after which the shear stress is proportional to the strain rate, i.e. a Bingham rheology (Robson, 1967; Hulme, 1974; Dragoni et al., 1986; Dragoni and Tallarico, 1994). For a Bingham fluid to flow downhill, it must form a layer thick enough for the shear stress at the base to exceed the yield strength. At the lateral boundaries of the flow, where the lava thickness is not enough to produce a basal shear stress larger than the yield stress, increasingly static regions of materials are left on the sides to form the initial lava flow levées. Hulme (1974) demonstrated that the yield strength, the density and the viscosity of the lava, together with the effusion rate and the terrain slope, control the depth and the width of the flow and the width of the initial levées, which are

\* Corresponding author. Fax: +39-051-4151498.  
E-mail address: [quarenì@bo.ingv.it](mailto:quarenì@bo.ingv.it) (F. Quarenì).

observed in both pahoehoe and aa flows. Furthermore, as found by Sparks et al. (1976), three other types of levées can be observed in the field and modify initial levées. Accretionary levées consist of piles of clinkers accreted to pahoehoe lava channels and welded together to form a steep, solid levée. In fully developed aa lava flows, rubble levées are formed as the front advances and the sides expand by debris avalanches. Finally, overflow levées are produced by lava flooding over already existing rubble levées. Lava flows are potentially dangerous if they reach inhabited or cultivated areas, and in order to avoid or reduce damage they can be diverted to sites where the exposed value is lower (Chester et al., 1985). The first attempt of lava flow deviation documented in historical chronicles (Gemmellaro, 1858) has been made at Etna, and dates back to 1669, when a group of citizens of Catania opened a breach in a lava flow levée using picks and axes. They succeeded, but made the inhabitants of Paternò very angry because the flow was then going toward their town. The people of Catania were forced to stop. More recently, many interventions of lava flow deviation were made in order to protect urban settlements, as at Mt. Etna in 1983 and 1992 (Barberi et al., 1993), but much attention is necessary when opening the levées in order to avoid even more severe damage. The levée can be opened using explosives, but because of the narrow margin of error allowed in locating the breach, it is often necessary to put the charges in place by hand. The levée is first excavated in order to narrow it, then holes are drilled through the thinned margin, and the charges are injected. However, the maximum safe-handling temperature of the explosives commonly used is around 200°C, and it is then necessary, in order to work safely, to know the temperature field in the lava flow levées. A sufficient time after their formation, the temperature in the lava flow levées is a conductive, steady-state field which satisfies the Laplace equation in an isotropic homogeneous medium, with boundary conditions prescribing the temperature at the interface between the levée and the air, and between the levée and the flowing lava. The solution is then depending only on the boundary conditions and the geometry of the levée.

In this paper, the steady-state temperature field is determined analytically by means of the conformal mapping technique for a triangular and a square levée, and numerically with a finite-element code for arbitrary shapes. The analytical and numerical solutions are compared, and the results are discussed, focusing on their potential application for civil protection purposes, although for a realistic solution, useful in practical situations, a more precise knowledge of the geometry and rock properties would be required.

## 2. The physical model

Due to the geometry and size of a lava flow, we assume that the length of the levée is much larger than its height and width, and we therefore consider a two-dimensional model on a vertical cross-section of the levée, in a Cartesian reference system, with the origin at the inner bottom of the levée. Assuming that the material forming the levée can be modeled as a thermally isotropic, homogeneous medium, endowed with properties that are not dependent on the temperature, the steady-state equation for conduction is the Laplace equation:

$$\frac{\partial^2 T}{\partial x^2} + \frac{\partial^2 T}{\partial y^2} = 0 \quad (1)$$

where  $T$  is the temperature,  $x$  and  $y$  are the horizontal and vertical coordinates. The lava flow levée, i.e. the portion of material where the crystallization in the magmatic suspension is sufficient to inhibit the motion, can be identified as the region where the temperature is below a certain value, above the solidus, which should be measured experimentally. However, due to the lack of data, the thermal model is applied here only to the solid portion, which we call 'levée' in the following. The boundary conditions then prescribe that the temperature is fixed at the levée/lava interface, equal to the solidus temperature of magma  $T_s$ , as well as the levée/air interface, equal to the air temperature  $T_a$ . In this paper, we assume  $T_s = 900^\circ\text{C}$ , appropriate to basaltic lava, and  $T_a = 30^\circ\text{C}$ . The assumption of steady-state temperature distribution implies that the model can

be applied only for times large enough after the levée emplacement. If  $d$  is the levée width and  $\chi$  is the thermal diffusivity of lava, steady-state conditions are achieved approximately after a time  $t = d^2/(8\chi)$  (Osizik, 1968), which is in the order of 1 day, for  $d$  equal to about 1 m and  $\chi$  equal to about  $10^{-6} \text{ m}^2 \text{ s}^{-1}$ . In the field, the inner margins of the levées are observed to be very abrupt and steep, very seldom subvertical, and the channel floor nearly flat, while the outer geometry shows more variability (Kilburn and Guest, 1993). We then assume an inner rectangular shape and take into account different outer geometries.

### 3. The analytical solution

The analytical solution of Eq. 1 is a harmonic function which must satisfy the given boundary conditions. Conformal mapping is a mathematical technique used to convert (or map) one mathematical problem and solution into another, and, under some very restrictive conditions, we can define a complex mapping function that will take every point in one complex plane and map it onto another complex plane. More precisely, a transformation  $w = f(z)$  is said to be conformal at a point  $z_0$  if  $f$  is analytic there and the derivative at  $z_0$  is non-zero. Thus, a transformation defined on a set is called a conformal mapping when it is conformal at each point in that set. Conformal mappings preserve magnitude and direction, with scaling given by the derivative. The Riemann theorem demonstrates that there exists a conformal mapping which allows to transform a domain  $D$  into a domain  $D'$ , provided that  $D$  has more than one frontier point.

Our aim is then to find a conformal mapping which transforms the levée cross-section into a half-space, and then to find the solution of Eq. 1 as a function of the complex variable  $z = x + iy$  with the following boundary conditions:

$$T(x, y = 0+) = \begin{cases} T_a & \text{for } x < 0 \\ T_s & \text{for } x > 0 \end{cases} \quad (2)$$

The harmonic function which satisfies Eqs. 1 and 2 is:

$$T(x, y) = T(z) = T_s - \frac{T_s - T_a}{\pi} \arg z \quad (3)$$

where  $z$  is a complex variable.

The conformal mapping which realizes the transformation of a half-space delimited by a polygonal-shaped surface into a half-space bounded by a plane surface is the Schwarz–Christoffel transformation (e.g. Floryan, 1987):

$$\frac{dw}{dz} = A(z - x_1)^{\alpha_1/\pi - 1} (z - x_2)^{\alpha_2/\pi - 1} \dots (z - x_n)^{\alpha_n/\pi - 1} \quad (4)$$

where  $A$  is a constant that may depend on  $x_i$ ,  $x_i$  are the points of the real axis of the  $z$  plane where the  $n$  vertices of the polygonal surfaces are mapped, and  $\alpha_i$  are the corresponding internal angles. Integrating Eq. 4, one obtains:

$$w(z) = f(z) = A \int_0^z (\zeta - x_1)^{\alpha_1/\pi - 1} (\zeta - x_2)^{\alpha_2/\pi - 1} \dots (\zeta - x_n)^{\alpha_n/\pi - 1} d\zeta + B \quad (5)$$

where  $B$  is a constant.  $A$  and  $B$  are calculated from the size, orientation, and position of the polygonal curve. It can be demonstrated that if one of the vertices of the polygonal surface is mapped to infinity, there exists an appropriate choice of the constant  $A$  that allows to cancel the corresponding term in Eqs. 4 and 5. The temperature field in the physical plane  $w$  can then be calculated as:

$$T(w) = T(f^{-1}(w)) = T(z) \quad (6)$$

#### 3.1. Triangular levée

Let us first consider a triangular-shaped levée, as it is sketched in Fig. 1A, with the vertices in the points  $Q(0,0)$ ,  $P(0, -v_P)$ , and  $R(-u_P, 0)$  in the plane  $w$ . The conformal mapping has to transform the point  $P$  of the  $w$  plane into the origin  $P'$  of the plane  $z$ , and the origin  $Q$  of the plane  $w$  into the point  $Q'$  of coordinates  $(v_P/2, 0)$  in the plane  $z$ . The point  $R$  of the plane  $w$  is mapped in the point  $R'(-\infty, 0)$  in the plane  $z$ . The vertices  $P$  and  $Q$  that have to be transformed by Eqs. 4 and 5 are then  $n=2$ , and the corresponding internal angles are  $\beta$  and  $3\pi/2$ . The derivative of the Schwarz–Christoffel mapping is then:

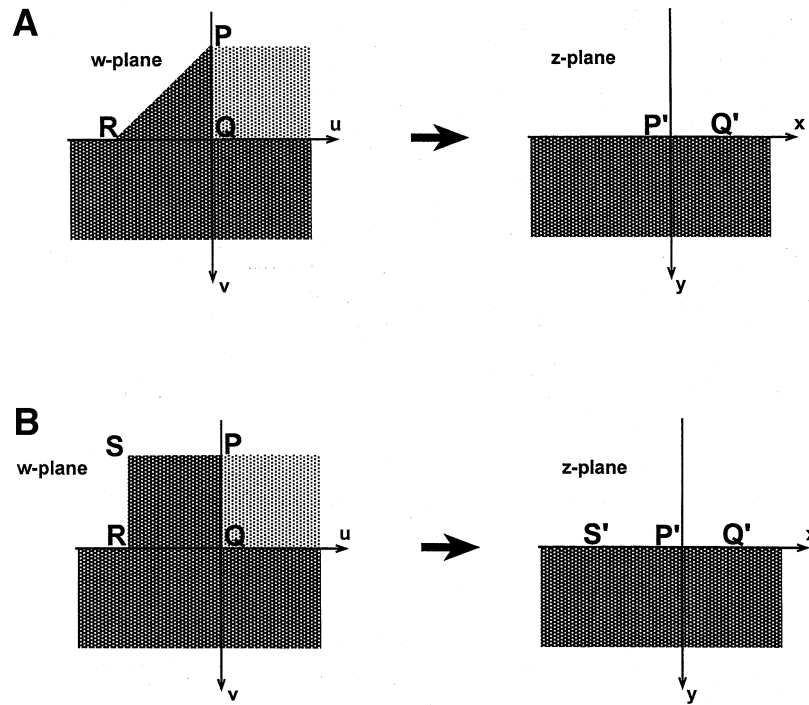


Fig. 1. Sketch of half of the real integration domain, i.e. the levée cross-section, in the  $w$  plane and of the conformal mapping to the  $z$  plane, for a triangular (panel A) and square (panel B) levée. The light-shaded area in the  $w$  plane represents the region occupied by the flowing lava.

$$\frac{dw}{dz} = kz^{\beta/\pi-1} (1-z)^{1/2} \quad (7)$$

where  $k$  is a constant. The conformal mapping is obtained by integrating Eq. 7:

$$w(z) = f(z) = k \int_0^z \zeta^{\beta/\pi-1} (1-\zeta)^{1/2} d\zeta + B \quad (8)$$

The integral of Eq. 8 can be calculated analytically for  $\beta = \pi/3$ , for  $\beta = \pi/6$ , and for  $\beta = \pi/4$ , and the constants are determined by requesting the mapping of the points P and Q into P' and Q', fixing for the present study  $v_P = 2$  m:

$$f(z) = \left( 4 \frac{\Gamma(11/6)i}{\Gamma(1/3)\sqrt{\pi}} \right) \left[ \frac{6}{5} z^{1/3} \sqrt{(1-z)} + \frac{9}{5} z^{1/3} F\left(\frac{1}{3}, \frac{1}{2}, \frac{1}{3}, z\right) \right] - 2i \text{ for } \beta = \frac{3}{2}\pi$$

$$\left( \frac{2\Gamma(5/3)i}{3\Gamma(7/6)\sqrt{\pi}} \right) \left[ \frac{3}{2} z^{1/6} \sqrt{(1-z)} + \frac{9}{2} z^{1/6} F\left(\frac{1}{6}, \frac{1}{2}, \frac{1}{6}, z\right) \right] - 2i \text{ for } \beta = \frac{\pi}{6}$$

$$\left( \frac{\Gamma(7/4)i}{\Gamma(5/4)\sqrt{\pi}} \right) \left[ \frac{4}{3} z^{1/4} \sqrt{(1-z)} + \frac{8}{3} E(\sin^{-1}(z^{1/4}), -1) \right] - 2i \text{ for } \beta = \frac{\pi}{4} \quad (9)$$

where  $F(a, b, c, z)$  is the hypergeometric Gaussian function of the variable  $z$  with the parameters  $a$ ,  $b$  and  $c$ , and  $E$  is the elliptic integral of the first kind.

### 3.2. Square levée

For a levée endowed with a square cross-section, as it is sketched in Fig. 1B, the number of vertices to be transformed is  $n=3$ . The transformation requiring that the points  $S(-u_P, -v_P)$ ,  $P(0, -v_P)$ , and  $Q(0, 0)$  are mapped into  $R'(-u_P, 0)$ ,  $S'(-u_P/2, 0)$ ,  $P'(0, 0)$ , and  $Q'(u_P/2, 0)$ , while the point  $R(-u_P, 0)$  is mapped into  $R'(-\infty, 0)$ , can be written as:

$$w(z) = f(z) =$$

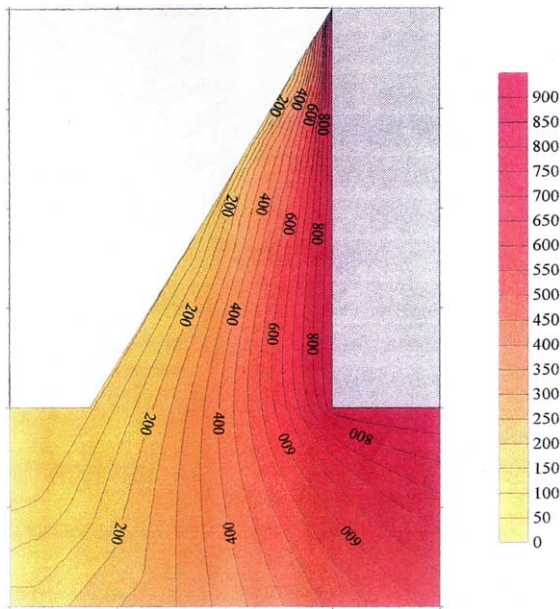


Fig. 2. Temperature field (in °C) obtained from the analytical model for a triangular levée with an internal angle at the top  $\beta = \pi/6$ .

$$k \int_0^z (\zeta + u_P/2)^{-1/2} \zeta^{-1/2} (\zeta - u_P/2)^{1/2} d\zeta + B \quad (10)$$

The integral is solved numerically for  $u_P = 2$  m and  $v_P = 2$  m.

#### 4. Results and discussion

The temperature field calculated with Eq. 9 for a triangular levée forming an internal angle at the top of  $\pi/6$ ,  $\pi/3$ ,  $\pi/4$ , and for a square levée are shown in Figs. 2–5, respectively. The height of the lava channel is 2 m in all the cases considered. From the solutions shown, we can infer a security depth at which the explosives can be placed, depending on the height above the lava flow basis.

The analytical method described in this paper allows one to calculate the temperature field rapidly, but only for simple geometrical shapes of the levée cross-section. Furthermore, the width of the lava flow is not accounted for in the conformal mapping method, since it is not possible to impose the existence of a central symmetry axis on the lava flow. Due to the lack of symmetry in Figs. 2–5 the horizontal temperature gradient does not vanish in the middle of the lava flow.

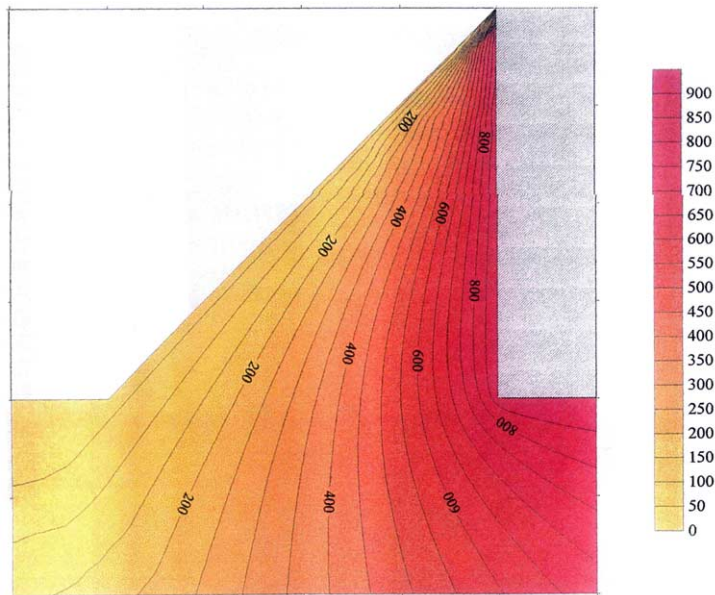


Fig. 3. Temperature field (in °C) obtained from the analytical model for a triangular levée with an internal angle at the top  $\beta = \pi/4$ .



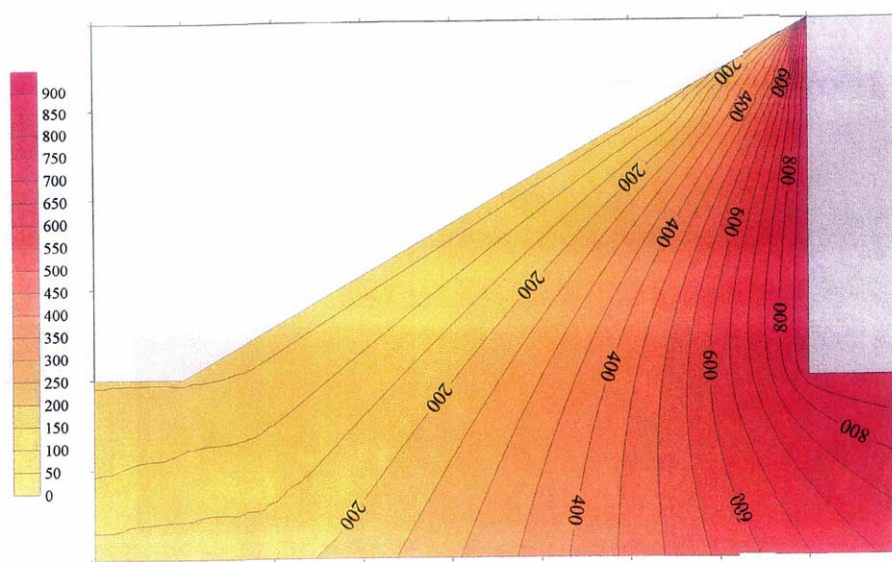


Fig. 4. Temperature field (in °C) obtained from the analytical model for a triangular levée with an internal angle at the top  $\beta = \pi/3$ .

In order to account for the width of the lava flow, and to find the temperature field in an arbitrarily shaped levée, we worked out a numerical model, solving the thermal conduction problem

by a finite-element method. The thermal analysis is therefore performed with the finite-element software [MARC \(2001\)](#). The grid used for finite-element calculations is obtained by meshing the in-

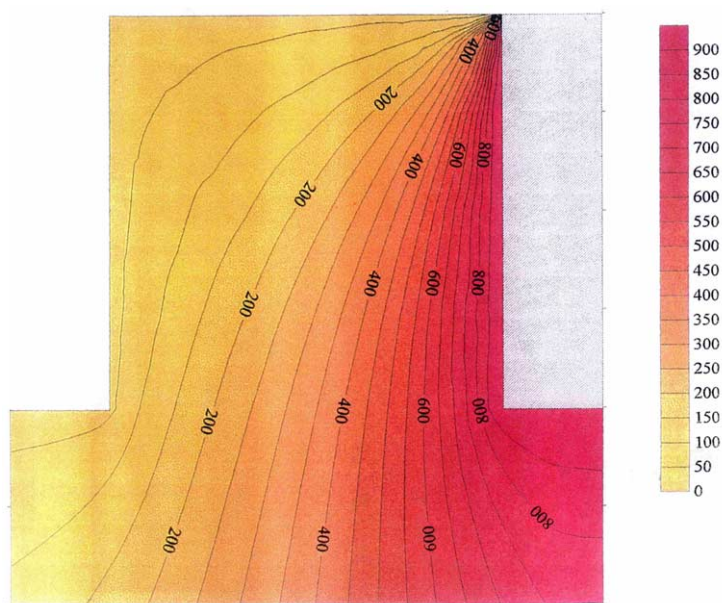


Fig. 5. Temperature field (in °C) obtained from the analytical model for a square levée.

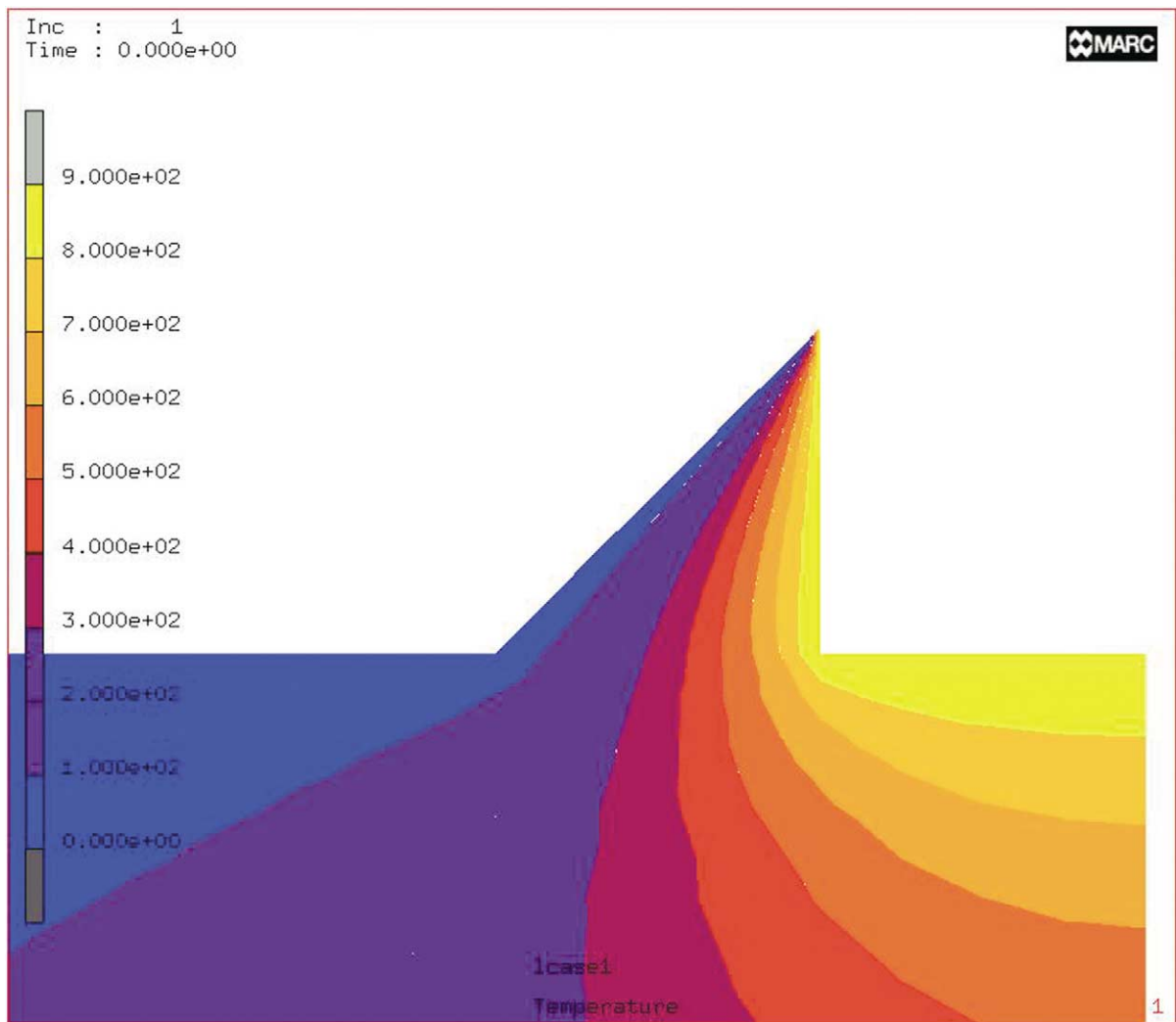


Fig. 6. Temperature field (in °C) obtained from the finite-element thermal analysis for a triangular levée with an internal angle at the top  $\beta = \pi/4$ .

tegration domain with two-dimensional, eight-node, iso-parametric, arbitrary quadrilateral and triangular elements written for planar heat transfer applications, which use biquadratic interpolation functions to represent the coordinates and displacements. Hence the thermal gradients have a linear variation, which allows for an accurate representation of the temperature field. The element conductivity is formed using nine-point Gaussian integration. As in the analytical model, the boundary conditions prescribe that the tem-

perature at the levée/lava interface is  $T_s = 900^\circ\text{C}$ , and that at the levée/air interface is  $T_a = 30^\circ\text{C}$ .

Figs. 6 and 7 show the temperature field calculated from the finite-element thermal analysis for a triangular (with a base angle of  $\pi/4$ ) and square levée cross-section; the height of the lava channel is 2 m, as in the cases treated with the analytical model, and the width of the channel is 4 m. The cases shown in Figs. 6 and 7 have to be compared with the analogous analytical solutions displayed in Figs. 4 and 5 respectively. The comparison be-

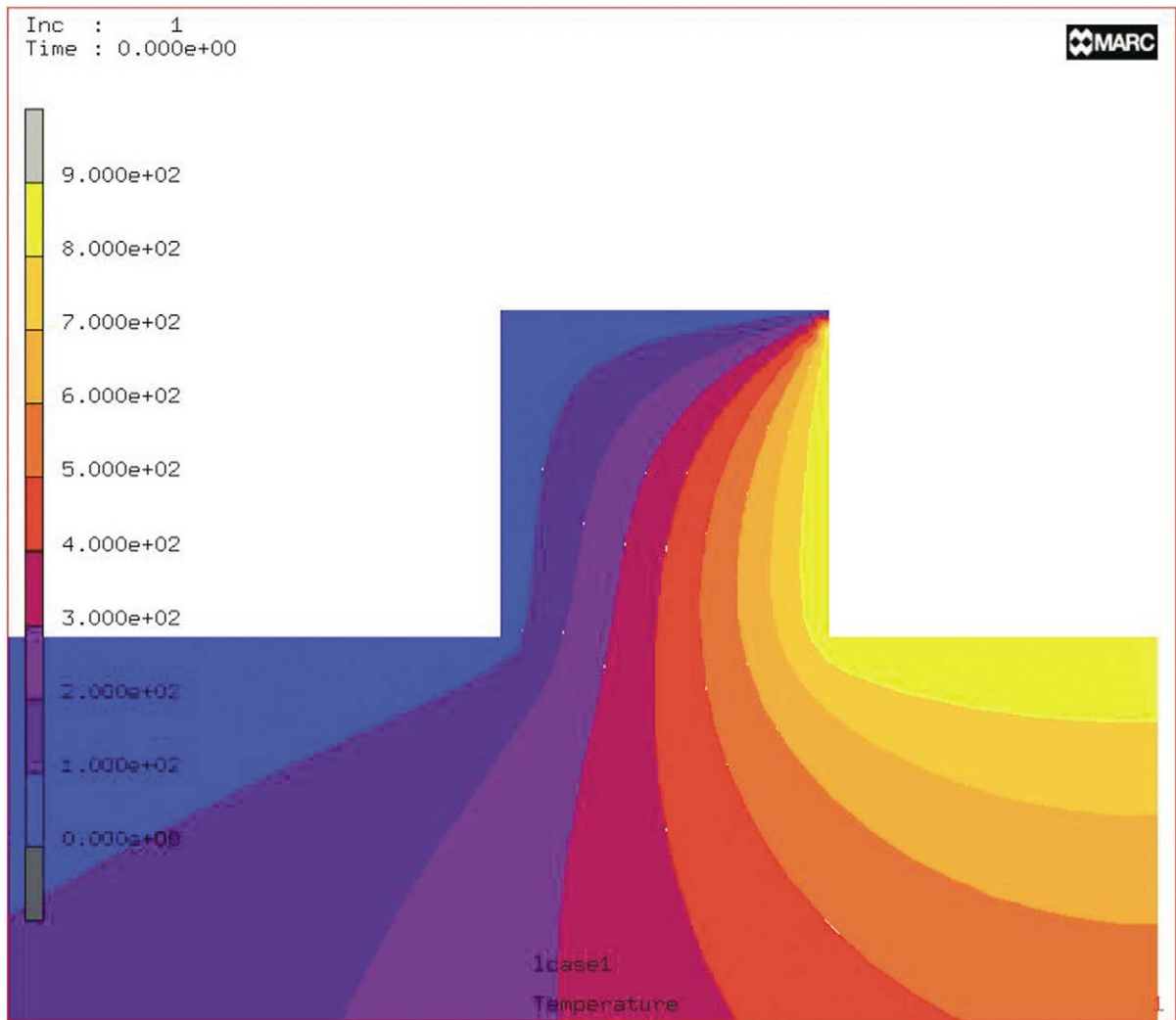


Fig. 7. Temperature field (in °C) obtained from the finite-element thermal analysis for a square levée.

tween the analytical and numerical temperature field shows a good agreement for the solutions in the levée, while it can be observed that the symmetry (flat isotherms beneath the center of the lava channel) is satisfied by the numerical results.

Fig. 8 shows the temperature field obtained from the numerical model for a trapezoidal levée, with height of 2 m, top basis of 1 m, and bottom basis of 2 m, which represents in a more realistic manner the shape of a levée. The isotherms exhibit a trend very similar to the case of the square

levée near the base, while the effect of the geometry becomes more evident near the top. A trapezoidal levée is also considered, but with a longer basis of 4 m, in order to mimic an excavated levée. The numerical solution for the thermal field is displayed in Fig. 9, where it can be observed that the safety depth for placing the explosives at the bottom is larger than in the previous cases, while smaller differences can be noticed at the top.

The results from the finite-element thermal analysis are summarized in Figs. 10–12, where the temperature is plotted across the levée as a



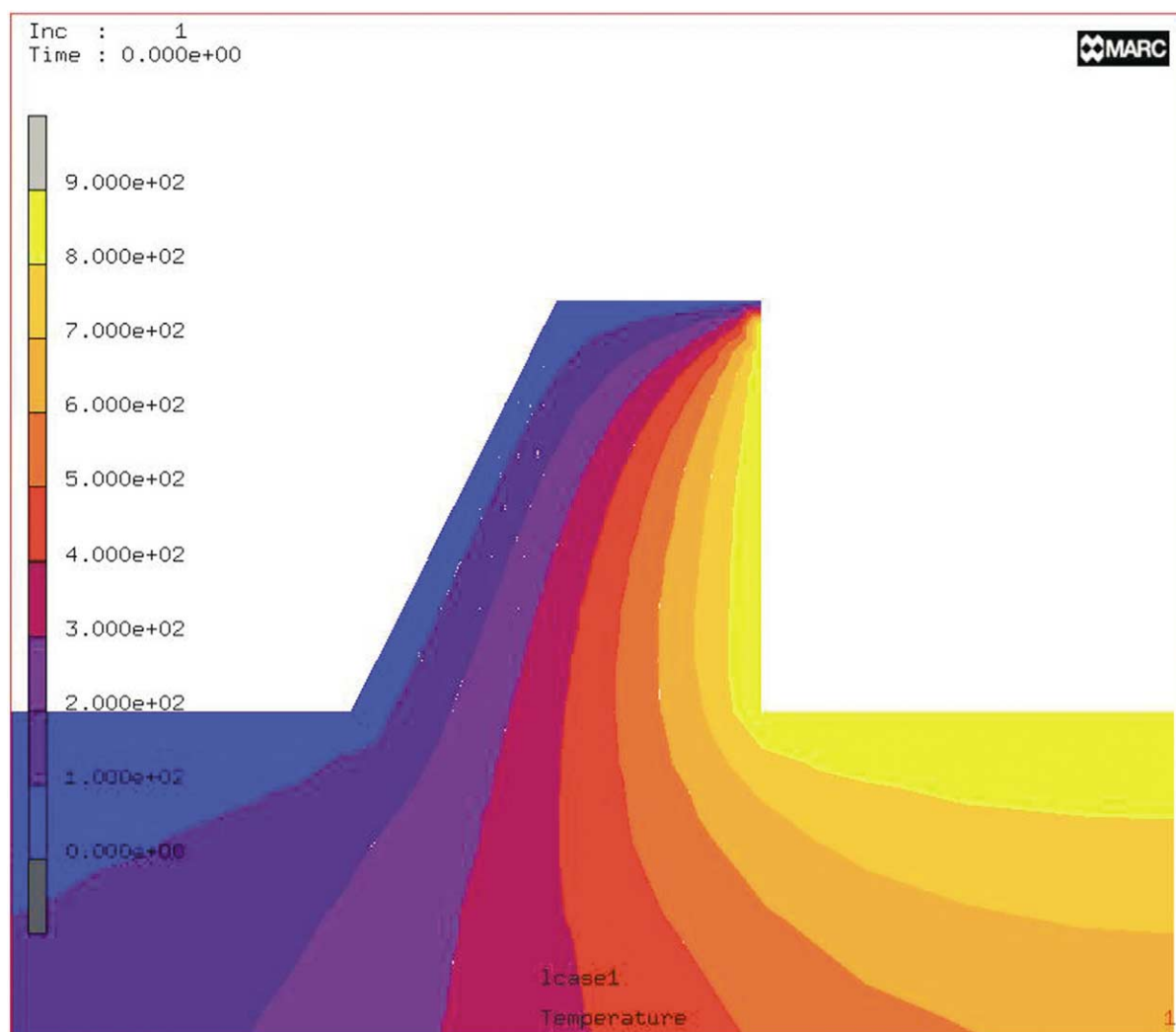


Fig. 8. Temperature field (in °C) obtained from the finite-element thermal analysis for a trapezoidal levée with a bottom basis of 2 m.

function of distance from the external boundary normalized to the levée thickness, at 0.25, 1, and 2 m below the top of the levée. These curves provide the safety depth for placing the explosives for the four cross-section shapes considered.

## 5. Concluding remarks

In this paper we calculate the steady-state temperature field in a lava flow levée, assuming that the levée cools by conduction, losing heat into the

atmosphere. The main purpose is to provide a model which can be applied, using a realistic geometry and rock properties, for civil protection purposes, providing information on the depth at which explosives can be safely placed inside the levée in order to deviate the lava flow.

The analytical model worked out in this paper is shown to provide reliable solutions for the steady-state temperature field in the levée, although the solutions lose their accuracy beneath the center of the lava channel, where the symmetry condition is not satisfied.

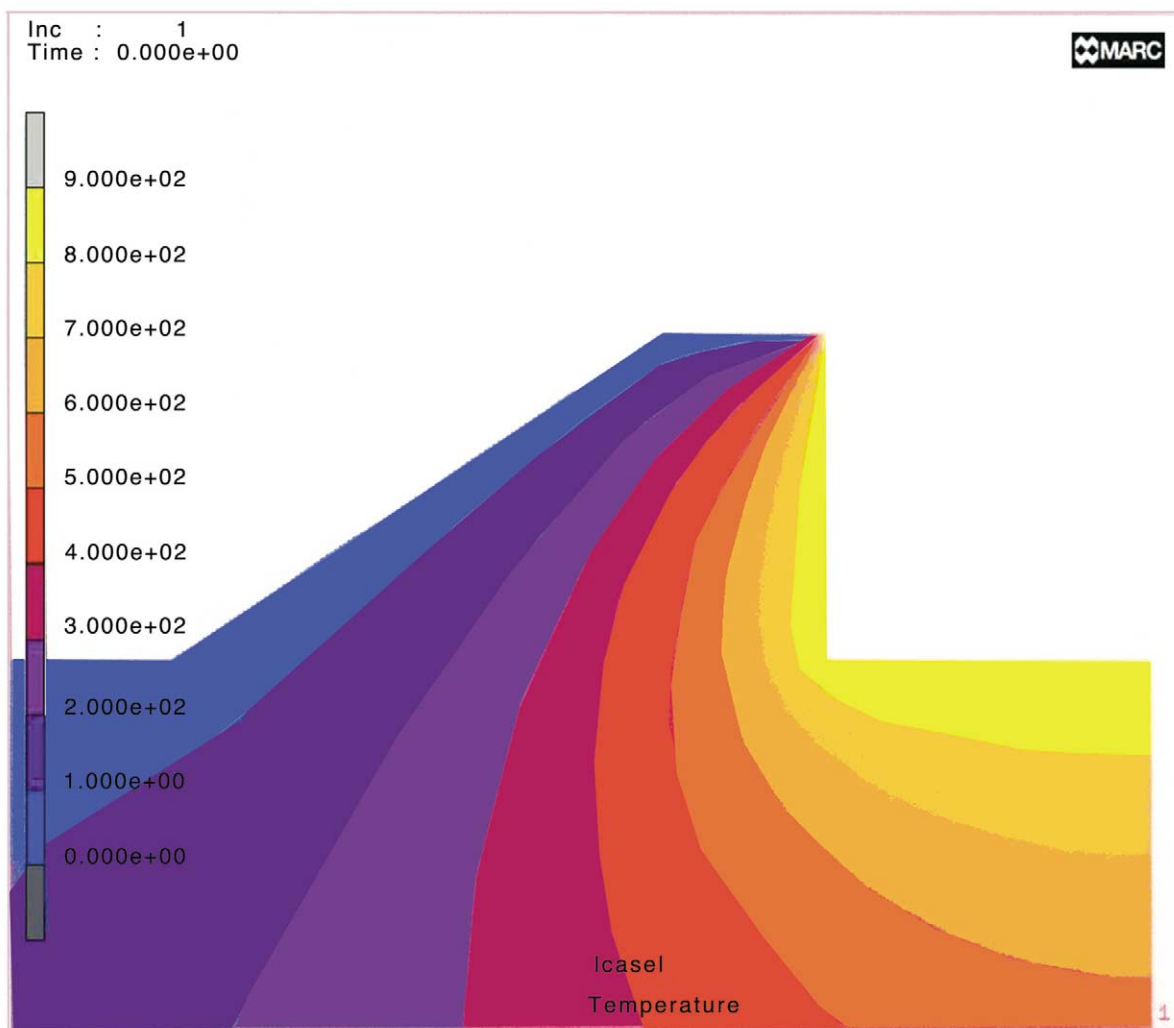


Fig. 9. Temperature field (in °C) obtained from the finite-element thermal analysis for a trapezoidal levée with a bottom basis of 4 m.

The finite-element thermal analysis allows one to calculate the temperature field in an arbitrarily shaped levée, satisfying the symmetry condition beneath the center of the lava channel, and accounting for the lava channel width.

The solutions obtained provide the safety depth at which the explosives can be placed to deviate a lava flow in order to prevent major damage: although we show here the benchmark cases of triangular, square, and trapezoidal levée cross-sections, this finite-element thermal model can be directly applied to any arbitrary,

irregular shape, and then used in practical situations.

The next objective of our future work is to provide transient solutions, in order to study the thermal evolution in a newly formed levée, as well as in a recently excavated levée.

#### Acknowledgements

This research was funded by the Gruppo Nazionale per la Vulcanologia, INGV.

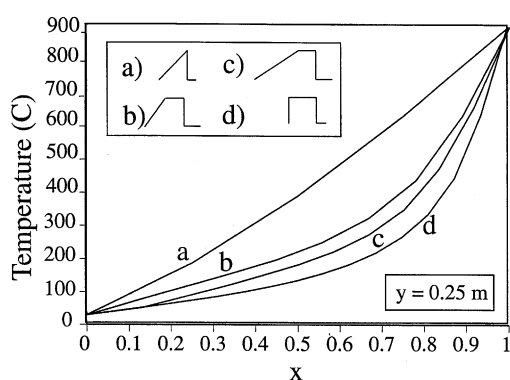


Fig. 10. Temperature (in °C) as a function of the distance  $x$  from the external boundary normalized to the levée thickness, at 0.25 m below the top of the levée, for a triangular, square and for the two trapezoidal shapes of the levée cross-section considered.

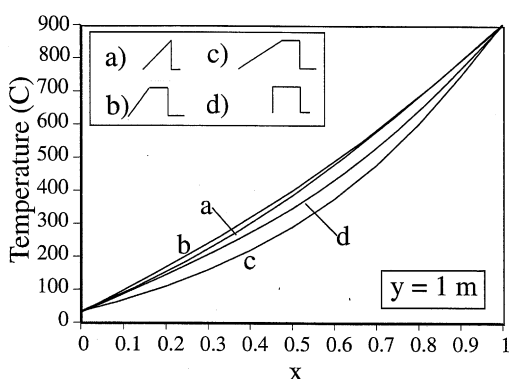


Fig. 11. Temperature (in °C) as a function of the distance  $x$  from the external boundary normalized to the levée thickness, at 1 m below the top of the levée, for a triangular, square and for the two trapezoidal shapes of the levée cross-section considered.

## References

- Barberi, F., Carapezza, M.L., Valenza, M., Villari, L., 1993. The control of lava flow during the 1991–92 eruption of Mount Etna. *J. Volcanol. Geotherm. Res.* 56, 1–34.
- Chester, D.K., Duncan, A.M., Guest, G.E., Kilburn, C.R.J., 1985. *Mount Etna: The Anatomy of a Volcano*. Chapman and Hall, London.

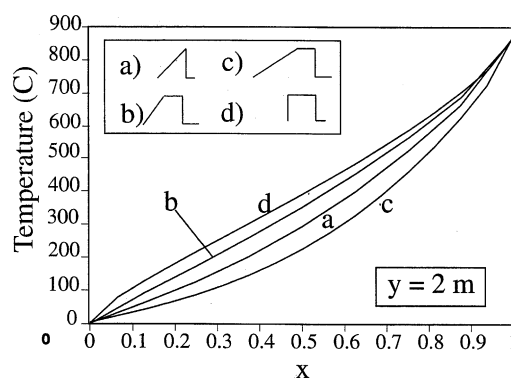


Fig. 12. Temperature (in °C) as a function of the distance  $x$  from the external boundary normalized to the levée thickness, at 2 m below the top (i.e. at the base) of the levée, for a triangular, square and for the two trapezoidal shapes of the levée cross-section considered.

- Dragonì, M., Bonafede, M., Boschi, E., 1986. Downslope flow models of a Bingham liquid: implications for lava flows. *J. Volcanol. Geotherm. Res.* 30, 305–325.
- Dragonì, M., Tallarico, A., 1994. The effect of crystallization on the rheology and dynamics of lava flows. *J. Volcanol. Geotherm. Res.* 59, 241–252.
- Gemmellaro, 1858. *La Vulcanologia dell'Etna*. Tipografia dell'Accademia Gioenia, Catania.
- Floryan, J.M., 1987. Schwarz-Christoffel transformations - a general approach. *J. Comput. Phys.* 72, 347–371.
- Hulme, G., 1974. The interpretation of lava flow morphology. *Geophys. J. R. Astron. Soc.* 39, 361–383.
- Kilburn, C.R.J., Guest, J.E., 1993. Aa lavas of Mount Etna, Sicily, in: Kilburn, C.R.J., Luongo, G. (Eds.), *Active Lavas*. University College London, London, chap.3.
- MARC Analysis Research Corporation, 2001. *MARC Reference Library*, Palo Alto, CA.
- Osizik, M.N., 1968. *Boundary-value Problems of Heat Conduction*. Int. Textbook Co., Scranton, PA.
- Pinkerton, H., Sparks, R.S.J., 1978. Field measurements of the rheology of lava. *Nature* 276, 383–385.
- Robson, G.R., 1967. Thickness of Etnean lavas. *Nature* 216, 251–252.
- Shaw, H.R., Wright, T.L., Peck, D.L., Okamura, R., 1968. The viscosity of basaltic magma: an analysis of field measurements in Makaopui Lava Lake. *Am. J. Sci.* 266, 224–225.
- Sparks, R.S.J., Pinkerton, H., Hulme, G., 1976. Classification and formation of lava levées on Mount Etna, Sicily. *Geology* 4, 269–271.